Large-amplitude internal wave generation in the lee of step-shaped topography

B. R. Sutherland
University of Alberta, Edmonton, Canada

Received 12 April 2002; accepted 6 June 2002; published 20 August 2002.

[1] Laboratory experiments show that as uniformly stratified fluid flows over a smoothly-varying step, two wave-like phenomena result: boundary-trapped lee waves, characterized by an undular shear layer downstream of the base of the step, and internal waves, which propagate vertically away from the step. The frequency of both types of waves is an approximately constant fraction of the buoyancy frequency. The frequency of internal waves is moderately smaller than lee waves if the step size is small but, if the step size is large, the frequencies match more closely. Thus nonlinear dynamics act so that internal waves are generated not by topography alone but also by flow over the boundary-trapped lee waves that act as "fluidic" hills. This new mechanism for internal wave generation may be an important factor in mixing over rough topography in the ocean. *INDEX TERMS:* 4544 Oceanography: Physical: Internal and inertial waves; 3384 Meteorology and Atmospheric Dynamics: Waves and tides; 3329 Meteorology and Atmospheric Dynamics: Mesoscale meteorology; *KEYWORDS:* internal waves, lee waves, rough topography

1. Introduction

[2] When a uniformly stratified fluid, characterised by constant buoyancy frequency N, flows with speed U over topography internal waves are generated if the forcing frequency is sufficiently small. Linear theory successfully predicts the characteristics of internal waves provided the aspect ratio of the topographic height, H, to width, L, is small. If the aspect ratio is larger, nonlinear effects are more important. In particular, large-amplitude waves are not necessarily "passively" generated; the waves can significantly change the flow field near the topography in a way that modifies the manner in which they are generated.

[3] The excitation of large-amplitude vertically propagating internal waves generated by an isolated (two-dimensional) hill has been examined in detail by way of theory [*Long*, 1953; *Smith*, 1985], numerical simulations [*Peltier and Clark*, 1979; *Peltier and Scinocca*, 1990] and laboratory experiments [*Rottman and Smith*, 1989; *Castro and Snyder*, 1993; *Bonneton et al.*, 1999]. These studies have identified conditions under which wave breaking occurs and have shown that severe downslope windstorms may occur ultimately in response [*Lilly*, 1971; *Lilly and Kennedy*, 1973; *Peltier and Scinocca*, 1990]. The complex density and wind structure of the atmosphere as well as strong topographic forcing both contribute to the nonlinear behaviour of the observed waves.

0094-8276/02/2002GL015321

[4] For a limited parameter range, a distinct wave phenomena has been observed in experiments [*Baines and Hoinka*, 1985]: a boundary-trapped lee wave. This is characterized by a stationary, undulating shear layer occurring horizontally downstream of topography. If sufficiently large amplitude, these lee waves can develop into rotors [*Scorer*, 1955; *Doyle and Durran*, 2002], a phenomenon that can constitute a severe hazard to air traffic [*Kuettner*, 1959]. Though the oceanic counterpart of these dynamics has not been observed directly, recent observations [*Ledwell et al.*, 2000; *Egbert and Ray*, 2000] suggest substantial mixing may occur due to dissipation of tidal energy near rough topography. Ledwell et al. have suggested that this mixing results from breaking internal waves, although the mechanism for generation of these waves from barotropic tides remains unclear.

[5] The purpose of this study is to examine under what circumstances boundary-trapped waves and vertically propagating internal waves are generated in the lee of flow over a smoothly varying topographic step. In this idealized study, there are two reasons for employing such a geometry. First, in the lee of a tall isolated hill of length L waves are generated both because of buoyancy restoring forces (returning stratified fluid driven up and over the hill to its equilibrium depth) and because of the adverse pressure gradient that develops in the lee. The step geometry enables us to ascertain unambiguously the extent to which large-amplitude waves are generated by the latter effect alone. Second, the step is the simplest representation of rough (discontinuous) topography that allows the examination of motions occurring on scales smaller than the roughness length.

[6] These experiments differ from classical studies of tank-scale internal wave modes [*Long*, 1955] in that we focus on the early development of quasi-steady waves which are not significantly influenced by the vertical and lateral tank boundaries. Using a recently developed laboratory technique that sensitively measures the frequency and amplitude of both lee and internal waves, we are able to examine the nonlinear coupling between the two phenomena.

2. Experimental Setup

[7] The experiments are performed in a 2 metre long glass tank as shown in Figure 1. The tank is filled with uniformly salt-stratified fluid, whose density decreases linearly with distance from the bottom of the tank so that the buoyancy frequency is constant. Experiments are run with N^2 ranging from 0.77 to 1.2 ± 0.05 s^{-2}.

[8] The spanwise-uniform model terrain floats on the surface. The approximately step-shaped terrain varies

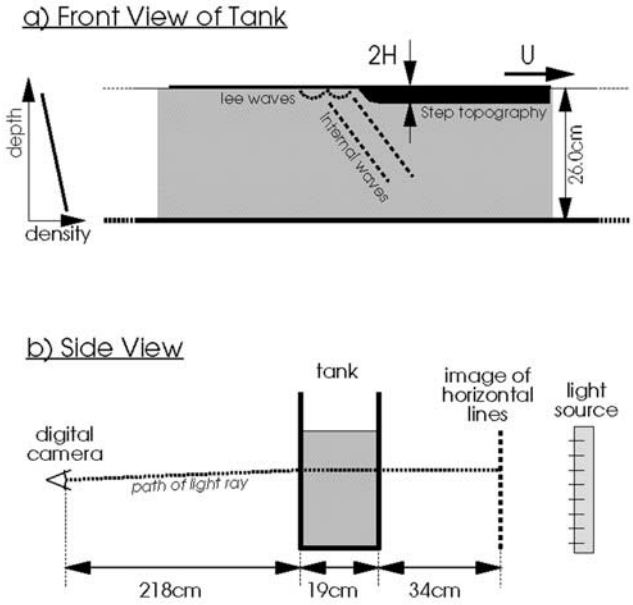

Figure 1. Set-up of the experiment. The model topography is towed at constant speed, U, along the top of a tank filled with salt-stratified water. Internal waves, which emanate downward from the topography (as illustrated schematically by the diagonal dotted lines in diagram a), are visualised by digitally recording how an image of horizontal lines is distorted when light passes through the fluid with time and space-varying index of refraction (diagram b).

sinusoidally over a half period from the top to the bottom of the step over a distance of 3.4 cm. This distance was chosen to be much smaller than typical wavelengths of the lee wave but not so small that vortex shedding would occur due to flow around a corner. Experiments are performed using two different step sizes with half-top-to-bottom heights of H = 0.65 and 1.3 cm The topography is towed by a high-torque motor at various speeds ranging from $U \simeq$ 0.78 to 3.32 ± 0.02 cm/s. Viewed in a frame of reference moving with the topography, the experiment models the generation of internal waves due to a constant flow over the step as characterised by a vertical Froude number $\mathrm{Fr}_v = U/NH$. The Reynolds numbers, based on flow speed and topographic height, are sufficiently large that the dynamics of boundary-layer separation do not significantly affect the wave dynamics. Indeed, theory predicts that stratification acts to accelerate the flow in the lee of the hill and suppress boundary-layer separation [*Marshall*, 2002], a result consistent with our observations.

[9] The waves themselves are visualised using a new technique called synthetic schlieren [*Dalziel et al.*, 2000]. The experiment is set up with a digital camera focussed on an illuminated grid of horizontal black lines positioned on the opposite side of the tank (see Figure 1b). The position of the lines appear to move when waves pass through the tank between the image and the camera. Provided the distortion of the lines is not too great and assuming the waves are uniform across the width of the tank, the changes in the density gradient can be computed from the displacement of the image. This non-intrusive method to measure wave amplitudes is preferred over standard particle tracking methods due to its high (pixel-scale) resolution and extreme sensitivity. Vertical displacements as small as 0.1 mm can be detected and those as small as 1 mm can be accurately measured everywhere in space and time. Unlike particle-tracking methods, which measure the flow in a slice through the fluid, schlieren measures the average motion across the span of the tank. However, this distinction is inconsequential when examining quasi-two-dimensional waves.

[10] For conceptual convenience, the images of experiments presented here are flipped upside down so that the waves appear to propagate upward from the hills. Because the density difference between the salt water at the top and bottom of the tank is small compared to the density of the water itself, the fluid is Boussinesq. Hence there is no dynamic difference between waves propagating downward from topography towed along the top of the tank and waves propagating upward from topography towed along the bottom of the tank [*Spiegel and Veronis*, 1960].

3. Results

[11] The flow immediately in the lee of the step establishes a quasi-steady state after one buoyancy period and the dynamics are examined over times between one and four buoyancy periods. This time range is sufficiently short that

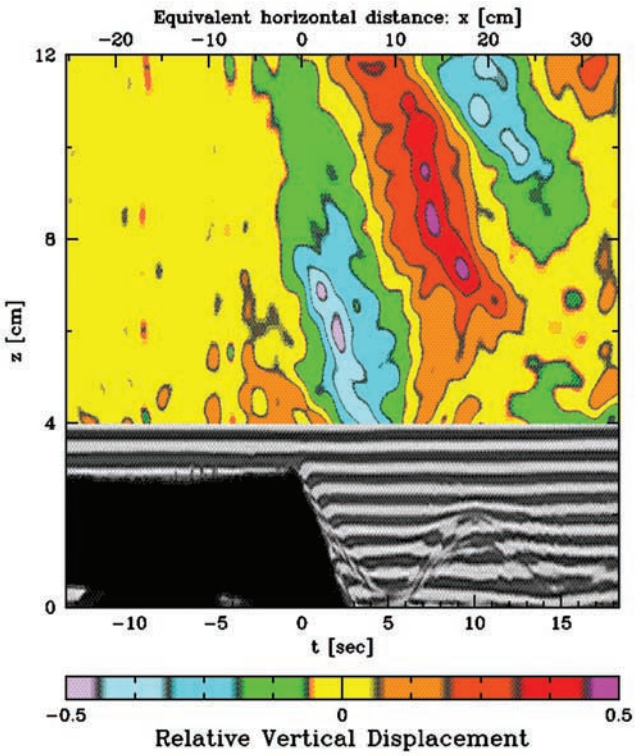

Figure 2. Vertical time series of lee waves and internal waves generated in the lee of a step in an experiment with Fr_v = 1.62. Explicitly, experimental parameters are U = 1.85 cm/s, H = 1.3 cm, and N = 0.88 s^{-1}. Below z = 4 cm, the image of the grid of horizontal black lines behind the tank is distorted due to the lee wave. Above z = 4,cm the distortion of lines is used to calculate the wave amplitudes, which are illustrated with colour contours representing values of the relative vertical displacement ξ/H.

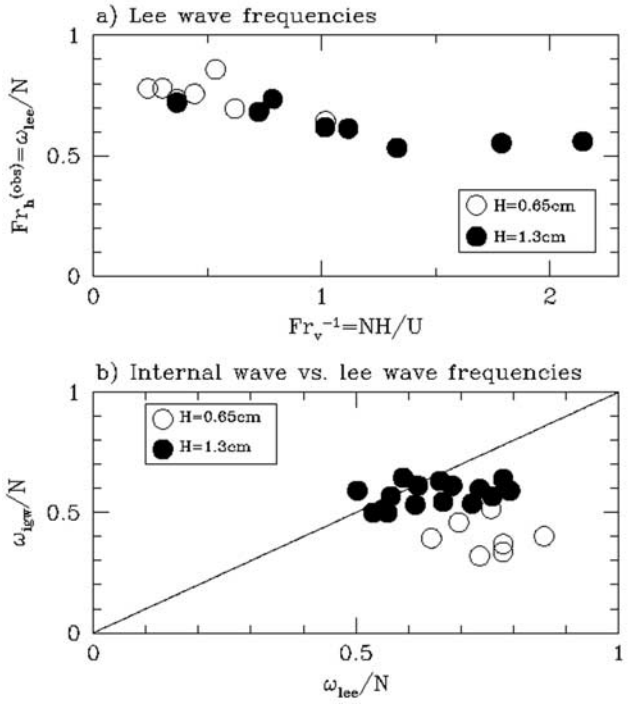

Figure 3. (a) Relative frequency of lee waves measured in experiments with H = 0.65 cm and 1.30 cm, N^2 = 0.8 s^{-2} and 1.4 s^{-2}, and U ranging from 0.7 to 3.5cm/s, as characterised by the inverse vertical Froude number, Fr_v^{-1}. (b) Comparison of internal waves and lee wave frequencies.

columnar modes do not significantly affect the dynamics. Over the parameter range discussed here, the flow immediately in the lee is found to be laminar. (In turbulent flows vortex shedding can be observed because the image of horizontal lines behind the tank becomes uniformly blurred.)

[12] Figure 2 shows that in the lee of the step the image of horizontal lines is greatly distorted. The distortion reveals a hump-shaped disturbance in the lee of the step. The hump, a "boundary-trapped" lee wave, is similar to that observed downstream of a single hill [*Baines and Hoinka*, 1985] except that here the lee wave is driven only by the pressure gradient established in the lee of the step. In small-amplitude, slow flow-speed experiments a second disturbance of still smaller amplitude trails the primary hump. In large-amplitude, fast flow-speed experiments, the flow in the lee of the first hump becomes turbulent, presumably as a consequence of shear instability.

[13] The lee wave is stationary with respect to the step. Its period with respect to the background flow is determined approximately from vertical time series images by measuring the time for the flow to travel from the top edge of the step to the first lee wave crest. The results, plotted in Figure 3a, show that the frequency ω_{lee} is an approximately constant fraction of N. In the linear regime ($Fr_v > 1$) $\omega_{lee} \simeq 0.75\,N$, and this decreases to moderately smaller values in the nonlinear regime.

[14] Figure 2 also shows that vertically propagating internal waves are generated above the lee of the step. Like the lee-waves, the relative frequency ω_{igw}/N is approximately constant but is generally smaller than ω_{lee}/N. However, Figure 3b shows that the frequencies match more closely if the waves are generated by a larger step. Thus the amplitude-dependent frequencies vary as a result of nonlinear resonant interactions with lee waves: large-amplitude internal waves are generated in part due to flow over the lee waves that act like "fluidic hills".

[15] Figure 4 confirms that nonlinear dynamics govern the generation and interaction of lee waves and internal waves. Figure 4a shows that the maximum vertical displacement of lee waves relative to the step size increases faster than linearly if the step size increases. The amplitude is generally larger in weakly stratified fluid and is limited approximately by C_aU/N, with $C_a \simeq 0.5$.

[16] Figure 4b shows that the internal wave amplitude is approximately equal to the lee wave amplitude.

4. Discussion and Conclusions

[17] Laboratory experiments show that both boundary-trapped lee waves and vertically propagating internal waves are generated for a wide range of Fr_v. The amplitudes of both waves are approximately equal and their frequencies relative to the buoyancy frequency match more closely if the step size is large. As in numerical simulations [*Laprise and Peltier*, 1989], our results demonstrate that the dynamics are governed by non-hydrostatic nonlinear effects. Here, however, the waves are not a consequence of wave breaking.

[18] This work demonstrates a new mechanism for internal wave generation in the lee of topography both in the atmosphere and ocean. In particular, the empirical data suggest an approach for parameterizing internal wave gen-

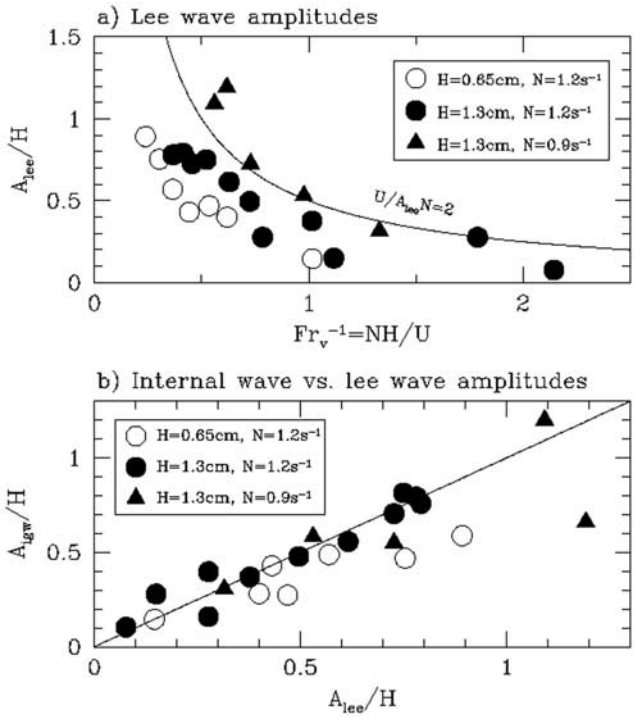

Figure 4. (a) Relative amplitudes of lee waves and (b) comparison of internal wave and lee wave amplitudes.

eration over rough topography in the deep ocean that does not presuppose a characteristic horizontal scale of the bathymetry. The simplest scaling for energy flux from waves generated by subcritical flow is $E_f \simeq \frac{1}{2}\rho_0 \kappa h^2 N U^2$, in which κ is the horizontal length scale and h^2 is the roughness. The experiments suggest that we set $\kappa = \omega/U \simeq C_\omega N/U$ with $C_\omega \simeq 0.75$ for $\mathrm{Fr}_v > 1$. Typical values for the deep ocean ($N \sim 10^{-5}$ s^{-1}, $U \sim 1$ cm/s) thus give $\kappa \simeq 2\pi/$(10 km). This is the same order as the optimal value of κ employed in a recent deep ocean internal wave parameterization scheme [*Jayne and St. Laurent*, 2001], in which κ was set to minimize the difference between modelled and observed tides. In rough regions of the ocean we assume the wave amplitude is limited by nonlinear effects in which case we take $h \simeq C_a U/N$, with $C_a = 0.5$. Therefore, the energy flux in rough regions of the ocean can be taken to be

$$E_f \simeq \rho_0 C_e U^3$$

where $C_e = C_\omega C_a^2/2 \simeq 0.1$. This estimate may be improved by performing more experiments to determine a better estimate of C_e and, in particular, C_a as a function of Fr_v.

[19] **Acknowledgments.** The author would like to thank D. Basnett for his technical assistance in setting up the experiments. This work has been supported by the Natural Sciences and Engineering Research Council of Canada.

References

Baines, P. G., and K. P. Hoinka, Stratified flow over two-dimensional topography in fluid of infinite depth: A laboratory simulation, *J. Atmos. Sci.*, *42*, 1614–1630, 1985.

Bonneton, P., O. Auban, and M. Perrier, Experiments on two-dimensional lee-wave breaking in stratified flow, in *Mixing and Dispersion in Stably Stratified Flows*, edited by P. A. Davies, pp. 505–520, Clarendon, Oxford, 1999.

Castro, I. P., and W. H. Snyder, Experiments on wave breaking in stratified flow over obstacles, *J. Fluid Mech.*, *225*, 195–211, 1993.

Dalziel, S. B., G. O. Hughes, and B. R. Sutherland, Whole field density measurements, *Experiments in Fluids*, *28*, 322–335, 2000.

Doyle, J. D., and D. R. Durran, The dynamics of mountain-wave-induced rotors, *J. Atmos. Sci.*, *59*, 186–201, 2002.

Egbert, G. D., and R. D. Ray, Significant dissipation of tidal energy in the deep ocean inferred from satellite altimeter data, *Nature*, *405*, 775–778, 2000.

Jayne, S. R., and L. C. St. Laurent, Parameterizing tidal dissipation over rough topography, *Geophys. Res. Lett.*, *28*, 811–814, 2001.

Kuettner, J., The rotor flow in the lee of mountains, *Tech. Rep. AFCRC-TN-58-626, G.R.D. Research Notes 6*, 20 pp., Air Force Cambridge Research Center, U.S. Air Force, 1959.

Laprise, R., and W. R. Peltier, The structure and energetics of transient eddies in a numerical simulation of breaking mountain waves, *J. Atmos. Sci.*, *46*, 565–585, 1989.

Ledwell, J. R., E. Montgomery, K. Polzin, L. St. Laurent, R. Schmitt, and J. Toole, Evidence for enhanced mixing over rough topography in the abyssal ocean, *Nature*, *403*, 179–182, 2000.

Lilly, D. K., Observations of mountain-induced turbulence, *J. Geophys. Res.*, *76*, 6585–6588, 1971.

Lilly, D. K., and P. J. Kennedy, Observations of a stationary mountain wave and its associated momentum flux and energy dissipation, *J. Atmos. Sci.*, *30*, 1135–1152, 1973.

Long, R. R., Some aspects of the flow of stratified fluids: A theoretical investigation, *Tellus*, *5*, 42–58, 1953.

Long, R. R., Some aspects of the flow of stratified fluids. III Continuous density gradients, *Tellus*, *7*, 341–357, 1955.

Marshall, D. P., pers. commun., 2002.

Peltier, W. R., and T. L. Clark, The evolution and stability of finite-amplitude mountain waves. Part II: Surface wave drag and severe downslope windstorms, *J. Atmos. Sci.*, *36*, 1498–1529, 1979.

Peltier, W. R., and J. F. Scinocca, The origin of severe downslope windstorm pulsations, *J. Atmos. Sci.*, *47*, 2853–2870, 1990.

Rottman, J. W., and R. B. Smith, A laboratory model of severe downslope windstorms, *Tellus*, *41A*, 401–415, 1989.

Scorer, R. S., The theory of airflow over mountains - IV. Separation of flow from the surface, *Quart. J. Roy. Meteor. Soc.*, *81*, 340 –350, 1955.

Smith, R. B., On severe downslope winds, *J. Atmos. Sci.*, *42*, 2597–2603, 1985.

Spiegel, E. A., and G. Veronis, On the Boussinesq approximation for a compressible fluid, *Astrophys. J.*, *131*, 442 –447, 1960.

B. R. Sutherland, Department of Mathematical and Statistical Sciences, University of Alberta, Edmonton, AB T6G 2G1, Canada. (bruce.sutherland@ualberta.ca)